

1 **Electronic Supplementary Information**

2

3 **Microwave selective effect: a new approach towards oxygen inhibition**  
4 **removal for highly-effective NO decomposition by microwave catalysis**  
5 **over BaMn<sub>x</sub>Mg<sub>1-x</sub>O<sub>3</sub> mixed oxides at low temperature under excess oxygen**

6 Wentao Xu, Jicheng Zhou\*, Yingpiao Ou, Yushang Luo, Zhimin You

7 Key Laboratory of Green Catalysis and Chemical Reaction Engineering of Hunan Province, School of  
8 Chemical Engineering, Xiangtan University, Xiangtan 411105, P.R.China

9

10 **S1. Experimental section**

11 *S1.1 Preparation of catalysts*

12 Ba(Ac)<sub>2</sub> (AR grade), Mn(NO<sub>3</sub>)<sub>2</sub> (AR grade) and Mg(NO<sub>3</sub>)<sub>2</sub> (AR grade) were primarily  
13 dissolved in deionized water according to the molar ratio of BaMn<sub>1-x</sub>Mg<sub>x</sub>O<sub>3</sub>  
14 (x=0,0.1,0.2,0.3,0.4). Citric acid and glycol were added into the aqueous solution, where the  
15 mole number of the complexing species were 1.25 times of metal ions including Ba<sup>2+</sup>, Mn<sup>2+</sup>  
16 and Mg<sup>2+</sup>. The aqueous solutions were stirred at 80 °C for 2.5 h to obtain spongy amorphous  
17 gels. The acquired gels were dried at 120 °C overnight and submitted to decomposition in  
18 air at 400 °C for 2 h and then calcined at 700 °C for 4 h.

19 For comparison, the BaMn<sub>0.9</sub>Mg<sub>0.1</sub>O<sub>3</sub>-1000 sample was calcined at 400 °C for 2 h and  
20 then at 1000 °C for 6 h.

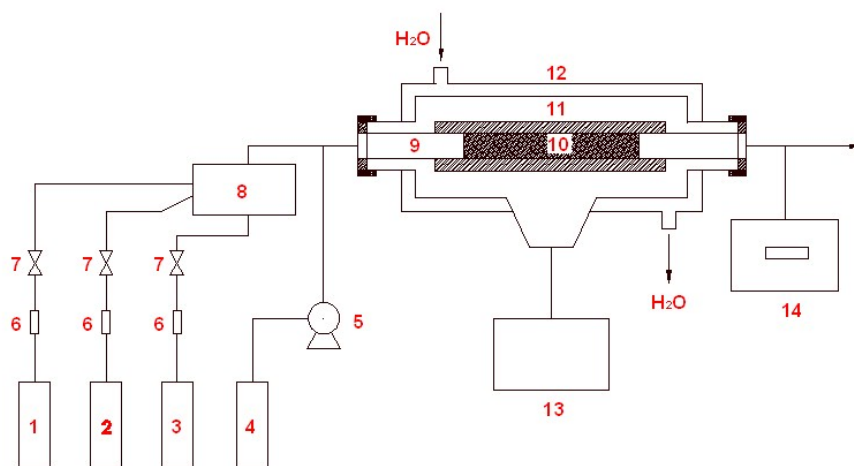
21 *S1.2 Catalysts Characterization*

22 The catalysts were analyzed by X-ray diffraction (XRD, Rigaku D/max-II/2500). The

1 working voltage and current were respectively 40 kV and 40mA, and Cu Ka radiation was  
2 employed.

### 3 *SI.3 Activity evaluation*

#### 4 *SI.3.1 Microwave reactor system*



5

6 **Fig. S1** Schematic diagram of microwave catalytic reactor system

7 1. NO; 2.O<sub>2</sub>; 3.N<sub>2</sub>; 4. Storage tank; 5. Metering pump; 6. Mass flow meter; 7. Valve; 8.Premixer; 9.  
8 Quartz reactor; 10. Fixed bed; 11. Thermal insulation; 12. Resonant cavity; 13. Microwave generator; 14.  
9 On-line NO<sub>x</sub> analyzer

10

11 A new microwave catalytic reactor system was developed to research the role of the  
12 microwave irradiation in a continuous flow of gas-solid catalytic reaction system. The  
13 experimental diagram is shown in Fig. S1. The reactor consisted of a microwave generator  
14 system and a reaction system. The microwave energy was supplied by a 2.45 GHz  
15 microwave generator where the power could be adjusted continuously in the range of 0-  
16 1000 W. The magnetron microwave source was connected through a rectangular waveguide  
17 to a resonant cavity (Φ28mm\*32mm, the space of microwave irradiation is not only the  
18 catalyst but the whole cavity). A quartz tube (i.d.10 mm and 540 mm in length) at the center

1 of the cavity was designed to perform the experiments. The catalyst was put in the middle of  
2 the reactor tube, and both ends were sealed with asbestos. The temperature of the reaction  
3 bed was provided by microwave thermal effect and was precisely measured by the modified  
4 thermocouple probe inserted to the catalyst bed.

5 Most commercially available microwave experimental apparatus are not well suited to  
6 investigate the microwave effects,<sup>S1,S2</sup> which may be attributed to the reasons as following:

7 (1) Applied microwave power may not be measured precisely.

8 (2) During the experiment, the reaction medium may not be irradiated by continuous and  
9 invariable microwave (pulsed or intermittent microwave input power do not satisfy  
10 invariable microwave power condition).

11 (3) Constant-temperature conditions may not be achieved, especially in the isothermal  
12 kinetic experiments.

13 (4) The reaction temperature may not be measured precisely because of the low quality  
14 temperature transducers or the temperature gradients formed in the reaction medium.

15 By contrast, the advantages of this reactor system are as follows:

16 (1) Continuously adjustable microwave power is range 0-1000W, and the frequency is  
17 2450 MHz.

18 (2) The temperature of the catalyst bed can be precisely controlled by microcomputer.

19 (3) The precise monitoring of the reaction temperature is important to investigate the  
20 microwave effects.<sup>S2</sup> Therefore, an improved thermocouple probe was inserted to the  
21 catalyst bed, which is used to precisely measure the temperature of the catalyst bed.

22 (4) Microwave source emits microwave and irradiates on the reaction tube, and the

1 circulating water system is set around the periphery of the furnace chamber to absorb the  
2 microwave that avoid damage to the magnetron caused by the reflected microwave, which  
3 could protect the magnetron and make microwave catalytic reaction able to run for a long  
4 time.

### 5 *SI.3.2 Activity tests*

6 The reactant gas mixtures were composed of NO (the molar fraction of 0.1%), O<sub>2</sub> (the  
7 molar fraction of 0-10.0%) and the balanced N<sub>2</sub>. The catalysts (2.0 g, 20-60 mesh) were  
8 used for each run and the reactant feed rates were fixed at W/F = 1 g s cm<sup>-3</sup>, where W and F  
9 were respectively the catalyst weight and the total flow rate of reactant gas (F=120 ml min<sup>-1</sup>).  
10 The concentrations of the NO and NO<sub>2</sub> in the outlet gas were analyzed through an online  
11 NO<sub>x</sub> analyzer (42C, Thermo Environmental Instruments Co., Ltd., U.S.). In addition, the  
12 analysis system has GC (Agilent 7890A) with a Poropak Q column and a thermal  
13 conductivity detector for the N<sub>2</sub>O analysis. In the microwave catalytic reaction mode  
14 (MCRM), N<sub>2</sub> was the principal product, NO<sub>2</sub> was the by-product, and N<sub>2</sub>O could not be  
15 detected. Therefore, the NO conversion and N<sub>2</sub> selectivity could be calculated by the  
16 formulas as follows:

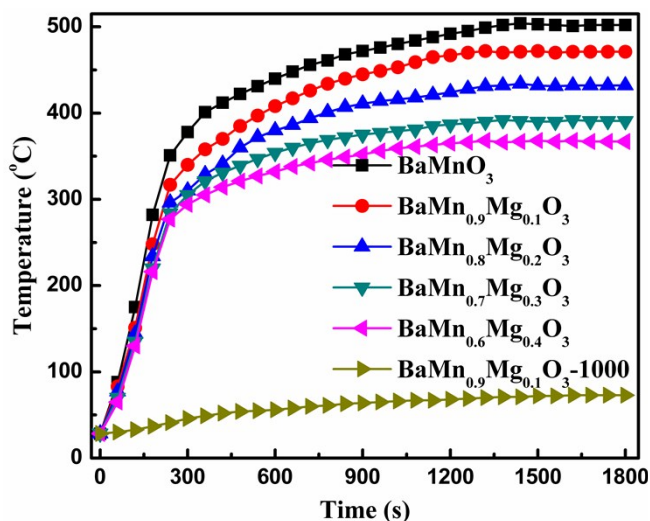
$$17 \quad X_{NO} = \frac{C_0(NO) - C_1(NO)}{C_0(NO)} \times 100\% \quad , \quad S_{NO} = \frac{C_0(NO) - C_1(NO) - C_1(NO_2)}{C_0(NO) - C_1(NO)} \times 100\%$$

18 ( $X_{NO}$  represents the NO conversion,  $S_{NO}$  represents the N<sub>2</sub> selectivity,  $C_0(NO)$  represents the NO  
19 concentration before the reaction,  $C_1(NO)$  represents the NO concentration after the reaction,  $C_1(NO_2)$   
20 represents the NO<sub>2</sub> concentration after the reaction)

21

22

## 1 S2. Results and discussion



2

3 **Fig. S2** Microwave heating profiles of  $\text{BaMn}_{1-x}\text{Mg}_x\text{O}_3$  and  $\text{BaMn}_{0.9}\text{Mg}_{0.1}\text{O}_3-1000$  at the microwave  
4 power of 150 W in the MCRM

5

6 The new microwave catalytic reactor is essentially different from the previous

7 microwave reactor, and the required reaction temperature of the catalysts relates to the

8 microwave absorbing properties of the catalyst itself. In another word, the catalyst must be

9 matched with microwave. Therefore, we investigated the microwave heating profiles of

10  $\text{BaMn}_{1-x}\text{Mg}_x\text{O}_3$  catalysts at the microwave power of 150W in the MCRM, and the results are

11 shown in Fig S2. The catalysts bed temperature increases with the microwave irradiation

12 time and then reaches to a stable temperature, and the microwave absorbing ability increases

13 with the increasing of the Mn content in  $\text{BaMn}_x\text{Mg}_{1-x}\text{O}_3$  (except for  $\text{BaMn}_{0.9}\text{Mg}_{0.1}\text{O}_3-1000$ ).

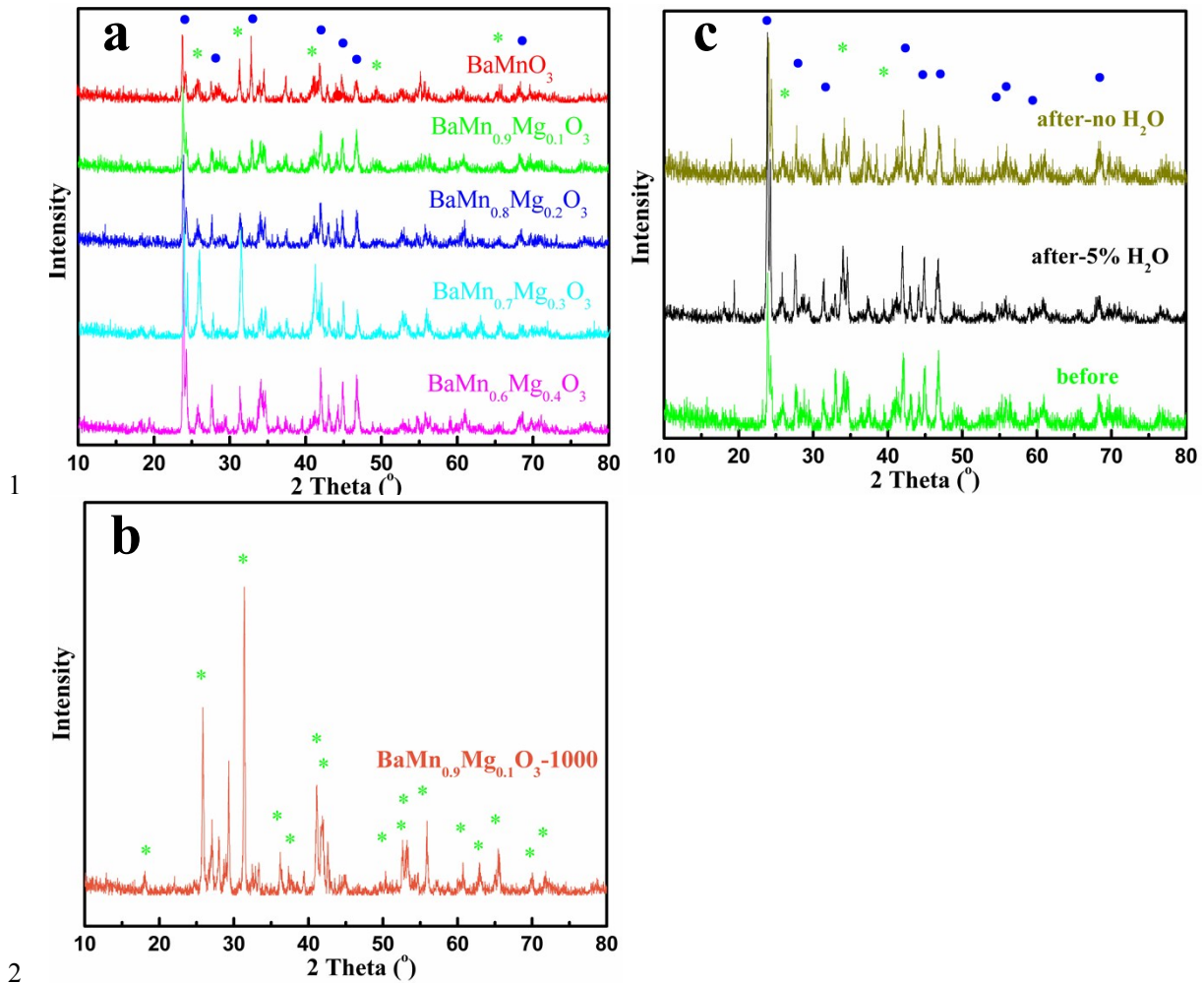
14 The stable bed temperature maintained at 502 °C of  $\text{BaMnO}_3$ , 471 °C of  $\text{BaMn}_{0.9}\text{Mg}_{0.1}\text{O}_3$ ,

15 432 °C of  $\text{BaMn}_{0.8}\text{Mg}_{0.2}\text{O}_3$ , 391 °C of  $\text{BaMn}_{0.7}\text{Mg}_{0.3}\text{O}_3$ , 367 °C of  $\text{BaMn}_{0.6}\text{Mg}_{0.4}\text{O}_3$  and 73

16 °C of  $\text{BaMn}_{0.9}\text{Mg}_{0.1}\text{O}_3-1000$  respectively at the microwave power of 150 W under

17 microwave irradiation for about 30min. In the following experiments, the catalyst bed

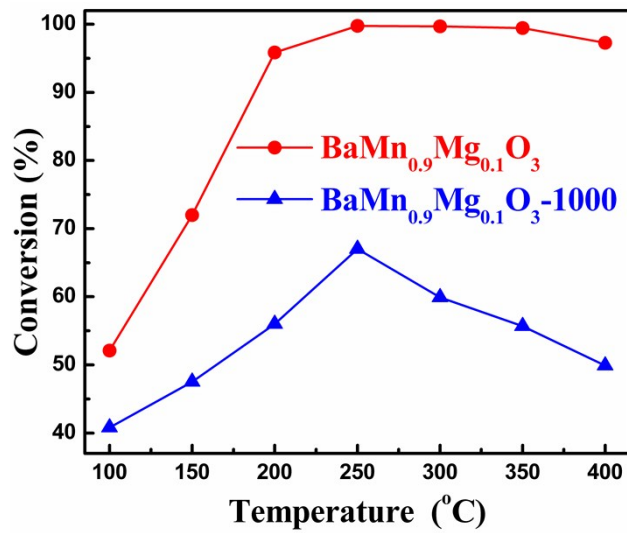
18 temperature in the MCRM was controlled by adjusting the microwave power.



1  
2  
3 **Fig. S3** XRD patterns of  $\text{BaMn}_{1-x}\text{Mg}_x\text{O}_3$  (a),  $\text{BaMn}_{0.9}\text{Mg}_{0.1}\text{O}_3$ -1000 (b), and  $\text{BaMn}_{0.9}\text{Mg}_{0.1}\text{O}_3$  before and  
4 after microwave reaction (c) (●  $\text{BaCO}_3$  and \*  $\text{BaMnO}_3$ )

5  
6 Fig. S3 shows the XRD patterns of the  $\text{BaMn}_{1-x}\text{Mg}_x\text{O}_3$  samples. Although all the  
7  $\text{BaMn}_{1-x}\text{Mg}_x\text{O}_3$  samples ( $x=0, 0.1, 0.2, 0.3, 0.4$ , calcined at  $700\text{ }^\circ\text{C}$ ) contain the diffraction  
8 peaks of  $\text{BaMnO}_3$  phase, the main diffraction peaks of all these  $\text{BaMn}_{1-x}\text{Mg}_x\text{O}_3$  samples can  
9 be assigned to  $\text{BaCO}_3$  phase, indicating that the  $\text{BaMn}_{1-x}\text{Mg}_x\text{O}_3$  samples are a kind of mixed  
10 oxides (Fig. S3a). However, the main diffraction peaks of the  $\text{BaMn}_{0.9}\text{Mg}_{0.1}\text{O}_3$ -1000 sample  
11 (calcined at  $1000\text{ }^\circ\text{C}$ ) can belong to the  $\text{BaMnO}_3$  phase (Fig. S3b), demonstrating that  
12  $\text{BaMn}_{0.9}\text{Mg}_{0.1}\text{O}_3$ -1000 possesses perovskite structure.

13



1

2 **Fig. S4** The influence of reaction temperatures on the NO conversion over BaMn<sub>0.9</sub>Mg<sub>0.1</sub>O<sub>3</sub>-1000 in the  
3 MCRM (Reaction conditions: molar fraction of O<sub>2</sub>, 5%; molar fraction of NO, 0.1%; W/F = 1 g s cm<sup>-3</sup>;  
4 and N<sub>2</sub> as the balance)

5

6

7

8

9

10

11

12

13

14

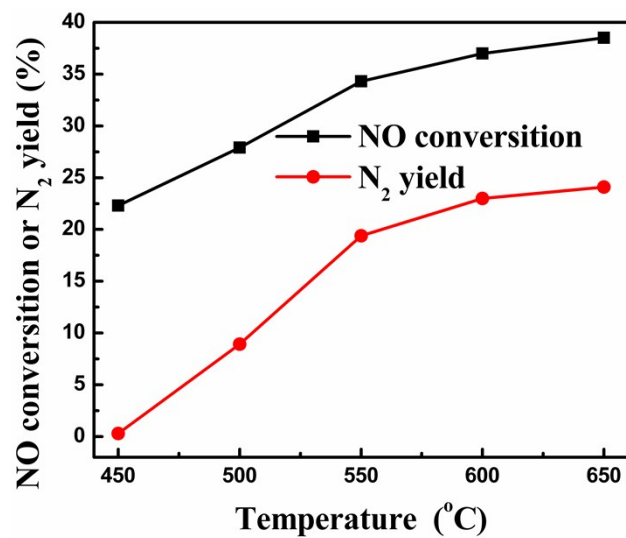
15

16

17

18

19



1  
2  
3  
4  
5  
6  
7  
8  
9  
10  
11  
12  
13  
14  
15  
16  
17  
18  
19  
20  
21  
22  
23  
24  
25  
26  
27  
28  
29  
30  
31  
32

**Fig. S5** The influence of reaction temperatures on the NO conversion and N<sub>2</sub> yield over BaMn<sub>0.9</sub>Mg<sub>0.1</sub>O<sub>3</sub> in the CRM (Reaction conditions: molar fraction of O<sub>2</sub>, 5%; molar fraction of NO, 0.1%; W/F = 1 g s cm<sup>-3</sup>; and N<sub>2</sub> as the balance)



1 **Table S1** The apparent activation energies (Ea') of direct catalytic decomposition of NO

Mode/Temperature conditions	Catalysts	Ea' (KJ/mol) <sup>a</sup>	Reference
Direct decomposition of NO	No catalyst	364	S3
CRM, 579-733K	Cu-ZSM-5	123	S4
MCRM, 200-250 °C	BaMnO <sub>3</sub>	15.5	This work
MCRM, 200-250 °C	BaMn <sub>0.9</sub> Mg <sub>0.1</sub> O <sub>3</sub>	27.8	This work
MCRM, 200-250 °C	BaMn <sub>0.8</sub> Mg <sub>0.2</sub> O <sub>3</sub>	23.9	This work
MCRM, 200-250 °C	BaMn <sub>0.7</sub> Mg <sub>0.3</sub> O <sub>3</sub>	24.2	This work
MCRM, 200-250 °C	BaMn <sub>0.6</sub> Mg <sub>0.4</sub> O <sub>3</sub>	11.6	This work
CRM, 873-923K	La <sub>0.87</sub> Sr <sub>0.13</sub> Mn <sub>0.2</sub> Ni <sub>0.8</sub> O <sub>3-δ</sub>	102	S5

<sup>a</sup> The apparent activation energies (Ea') were calculated by Arrhenius equation; The first-order with respect to NO was used to calculate kinetic data.<sup>S6</sup>

2

3

4

5

### 6 **S3. References:**

7 (S1) C. O. Kappe, B. Pieber and D. Dallinger, *Angew. Chem. Int. Ed.*, 2013, **52**, 1088.

8 (S2) B. Ergan and M. Bayramoglu, *Ind. Eng. Chem. Res.*, 2011, **50**, 6629.

9 (S3) H. Bosch and F. Janssen, *Catal. Today*, 1988, **2**, 369.

10 (S4) V. Tomasic, Z. Gomzi and S. Zrnecic, *Appl. Catal., B*, 1998, **18**, 233.

11 (S5) C. Tofan, D. Klvana and J. Kirchnerova, *Appl. Catal. A*, 2002, **226**, 225.

12 (S6) T. Yasutake, H. Tomohiro and K. Shuichi, *J. Chem. Soc., Faraday Trans.*, 1998, **94**,

13 1887.